Available online at www.sciencedirect.com
ScienceDirect
Journal of the European Ceramic Society 27 (2007) 41–45
www.elsevier.com/locate/jeurceramsoc

Fabrication of alumina-based ceramic foams utilizing superplasticity

Akira Kishimoto *, Mako Obata, Hiroshi Asaoka, Hidetaka Hayashi

Division of Chemistry and Biochemistry, Graduate School of Natural Science and Technology, Okayama University, 3-1-1 Tsushima-naka, Okayama 700-8530, Japan

Received 24 October 2005; received in revised form 28 February 2006; accepted 11 March 2006
Available online 3 July 2006

Abstract

Model ceramic foams were fabricated by expanding once-sintered dense shells utilizing the superplastic deformation of alumina dispersed with 3 mol% yttria-stabilized zirconia (3YSZ) or magnesia. The grain growth of alumina was suppressed by adding 3YSZ and the resultant grain size and amount of dispersion were closely related to the total porosity. Total porosity of the ceramic foam depended on the grain size and their distributions irrespective of the size of starting powders.

Keywords: Ceramics; Insulators; Grain size; Al_2O_3; Foams; Superplasticity

1. Introduction

We have already fabricated ceramic foam by expanding a once-sintered dense shell utilizing the superplastic deformation of 3 mol% yttria-stabilized zirconia.[1] The conventional solid-state processing of porous ceramics includes the partial-sintering method[2] and pore-forming inclusion method.[3] In liquid phase processing, an air bubble can easily be introduced into the precursor slurry or gel. Before the solidification process, the organic or liquid components evaporate, and porous ceramics that simultaneously have high porosity and high closed pore ratio are rarely attained, similar to solid-state ceramics processing.[4]

Sintering after foam introduction reduces the porosity because the sintering process inevitably involves the exclusion of pores. Consequently, the conventional porous ceramics process or sintering of a foamed precursor either results in insufficient sintering while maintaining porosity or improved inter-grain bonding at the expense of porosity.[5]

Similar to plastic and metal foams, highly reliable ceramics with greater porosity might be fabricated using inorganic melts. However, the formation of porous ceramics at above their melting points (2720 °C in the case of zirconia ceramics) has not been found practicable.

In our ceramics, the foaming processing is carried out after sintering; consequently, there is no degradation in inter-gain bonding and a high porosity is compatible with high structural reliability. Furthermore, the powder compaction process is simple and the foaming occurs during heating at the usual sintering temperatures under ambient pressures.

Compared with conventional porous ceramics fabricated with insufficient sintering, solid-state foamed ceramics have dense pore walls resulting in the favorable insulation of heat, gas and sound, in addition to their superior structural properties.

Superplasticity has been reported in several ceramics, which typically have fine grains, including covalently bonded silicon nitride[6] and super-conductive $YBa_2Cu_3O_{7-d}$ (YBCO).[7] However, the only report on superplasticity foaming is our report on 3 mol% yttria-stabilized zirconia (3YSZ).[1] Superplastic alumina, a more widely used ceramic, has already been reported in 3YSZ-dispersed,[8–11] MgO-dispersed[12–17] or 3YSZ + MgO-dispersed[18–20] systems. In this study, we successfully fabricated alumina-based ceramic foams after sintering by improving the superplasticity using several reported methods.

2. Experimental procedure

In order to demonstrate ceramic foaming following the sintering process, macroscopic single foams were fabricated using a method similar to that for 3YSZ.[1]

Alumina powders (AKP-15 to -53, Sumitomo Chemical, Tokyo, Japan) with various added amounts of 3YSZ or mag-

* Corresponding author. Tel.: +81 86 251 8069; fax: +81 86 251 8069.
E-mail address: kishim-a@cc.okayama-u.ac.jp (A. Kishimoto).

0955-2219/$ – see front matter © 2006 Elsevier Ltd. All rights reserved.
doi:10.1016/j.jeurceramsoc.2006.03.002

nesia (MgO) to enhance their superplasticity were used as the matrix. Silicon carbide was chosen as a high-temperature foam agent that decomposes to evaporate at high temperatures. First, 0.1 g of silicon carbide powder (Grade-UF, Ibiden, Aichi, Japan) was pressed into pellet in a Φ 10-mm die under 30 MPa. About 4 g of alumina-based powder was weighed. Half of the alumina-based powder, the compressed silicon carbide powder, and the remaining half of the alumina-based powder were put in a Φ 20-mm steel die and pressed uniaxially at 30 MPa for 1 min, and then hydrostatically at 200 MPa for 1 min. The resultant powder compacts were heated to 1600 °C at a rate of 800 °C/h, kept at that temperature for 4 or 8 h, and then cooled.

In order to evaluate the effects of the kind and amount of additive and the grain size of the starting powders, the other fabrication conditions were fixed, including the kind and amount of foaming agent, and the powder compaction and heating programs.

As additives to the alumina matrix powder, 3YSZ (TZ-3Y, average grain size: 0.05 μm, Tosoh, Tokyo, Japan) or magnesia (MO-V01P, average grain size: 0.05 μm, Ube Material Industry, Yamaguchi, Japan) were tested. For the 3YSZ-dispersed matrix, the effect of the amount added on the foaming characteristics was examined.

In order to evaluate the influence of the grain size of the starting powders, four different sized alumina powders (AKP-53, AKP-30, AKP-20 and AKP-15, Sumitomo Chemical, Tokyo, Japan) were processed in the same manner. Their median sizes were 0.2, 0.4, 0.5 and 0.6 μm, respectively, and each powder was named after its median size, e.g., "0.2-μm powder".

The external dimensions of the alumina-based ceramic foams, such as foam height and foam diameter, were measured using calipers. The apparent density of the outer shell and of the entire ceramic foam was measured using Archimedes' method with water as the medium. The porosity of the ceramic foam was estimated from the apparent density of the ceramic foam and the relative density of the outer shell. The fracture surface of the outer shell was polished to 9-μm diamond paste, thermally etched at 1500 °C for 30 min, and subjected to scanning electron microscopy (SEM). The sizes of approximately 100 ceramic grains were calculated using the code method and their distribution was evaluated. Crystalline phases that formed on the inner and outer sides of the shell were identified using an X-ray diffraction method (XRD) with Cu Kα radiation.

Table 1
The external sizes and porosities of the foams heat treated at 1600 °C for 8 h

Foam matrix	3YSZ	Alumina + 3YSZ	Alumina + MgO
Foam height (total height − pellet thickness) (mm)	5.3	6.0	3.5
Foam diameter (mm)	14.8	16.4	17.2
Relative density of the foam shell (%)	99	96	89
Total porosity (%)	30	36	16

3. Results and discussion

Fig. 1 shows photographs of ceramic foams made using (a) 3YSZ, (b) alumina + 3YSZ (30 mol%) and (c) alumina + MgO (30 mol%) as the matrix. We have already reported the fabrication of ceramic foams following sintering using 3YSZ.[1] As indicated in the photographs, alumina-based ceramic foams can be formed using superplasticity to facilitate by the dispersoids.

The external sizes and porosities of the foams are summarized in Table 1. Compared with zirconia-based foams, the alumina-based foams are characterized by low transverse shrinkage. Furthermore, the relative density of the outer shell in alumina-based foams is lower (<96%) than that of zirconia-based foams (almost 100%). Density degradation was thought to occur during the superplastic deformation because no abnormal grain growth was observed in the microstructure and the sinterability of the starting powder was favorable. It is widely known that grain orientation[10] and crack generation[19] occur in alumina-based ceramics on superplastic deformation. A coarse portion should

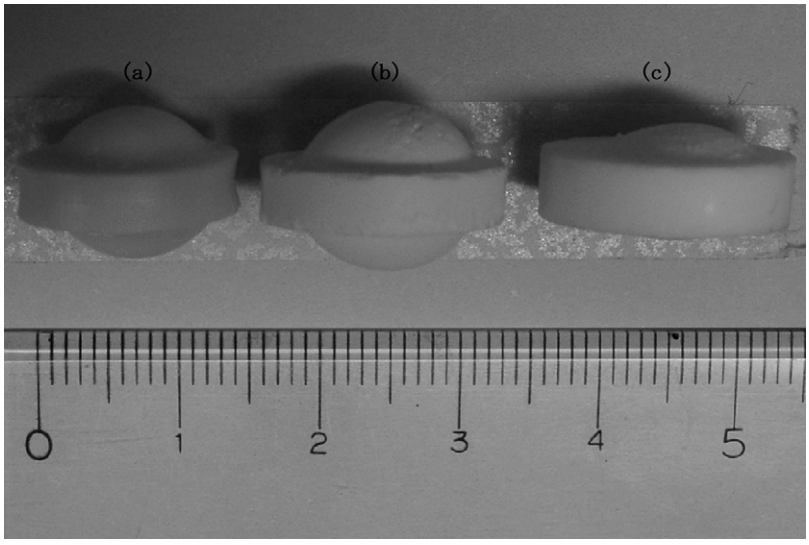

Fig. 1. Side view of macroscopic ceramic foams fabricated by foaming after sintering of alumina-based matrix with silicon carbide as a foam agent.

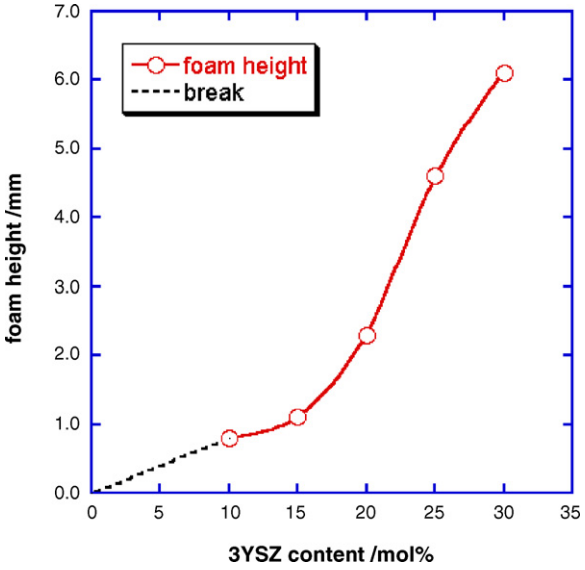

Fig. 2. Foam height of alumina-based mono-foams with various amount of 3YSZ, heat-treated at 1600 °C for 8 h.

be formed, although no crack generation was observed in our foams.

The foam size of magnesia-dispersed alumina is very small. Hiraga et al.[19] reported that the ductility of magnesia-dispersed alumina is inferior to that of 3YSZ-dispersed alumina. The small foaming size of magnesia-dispersed alumina is ascribed to its low ductility.

This study focused on the alumina/3YSZ system, and we investigated the relationship between foam height and grain size by changing the amount of 3YSZ or the powder size of alumina, while maintaining the other process conditions.

First, foam height was measured for alumina-based foams dispersed with various amounts of 3YSZ. The results are shown in Fig. 2(a). Ceramic foams can be fabricated without crack generation by adding more than 10 mol% 3YSZ. The foam height increased with the amount of 3YSZ. The dispersion of zirconia in alumina is known to suppress grain growth, resulting in improved superplasticity.[8] Fig. 2(b) shows the heating time dependent total porosity, shell wall thickness and the relative density of the shell of 30 mol% of 3YSZ dispersed alumina foam. The relative density of the shell exceeded 93% of theoretical within 4 h heating. On the other hand, total porosity gradually increased from 34% at 4 h heating to 41% at 16 h heating, suggesting the expansion of closed pore after densification. Accompanied by this pore evolution, shell wall thickness decreased from 1.8 to 1.1 mm.

In order to confirm the suppression of grain growth on the addition of zirconia particles, the fracture surfaces of the foam walls were observed using SEM. Fig. 3(a)–(c) are SEM photographs of 10, 20 and 30 mol% zirconia-dispersed alumina foams, respectively. The dispersed zirconia particles, which appear relatively white, are located at the grain boundaries of the alumina. Note that the size of the zirconia remains constant irrespective of the amount dispersed. The foam shells appear dense and we cannot find cracks, which have been reported in very deformed alumina-based ceramics.[19]

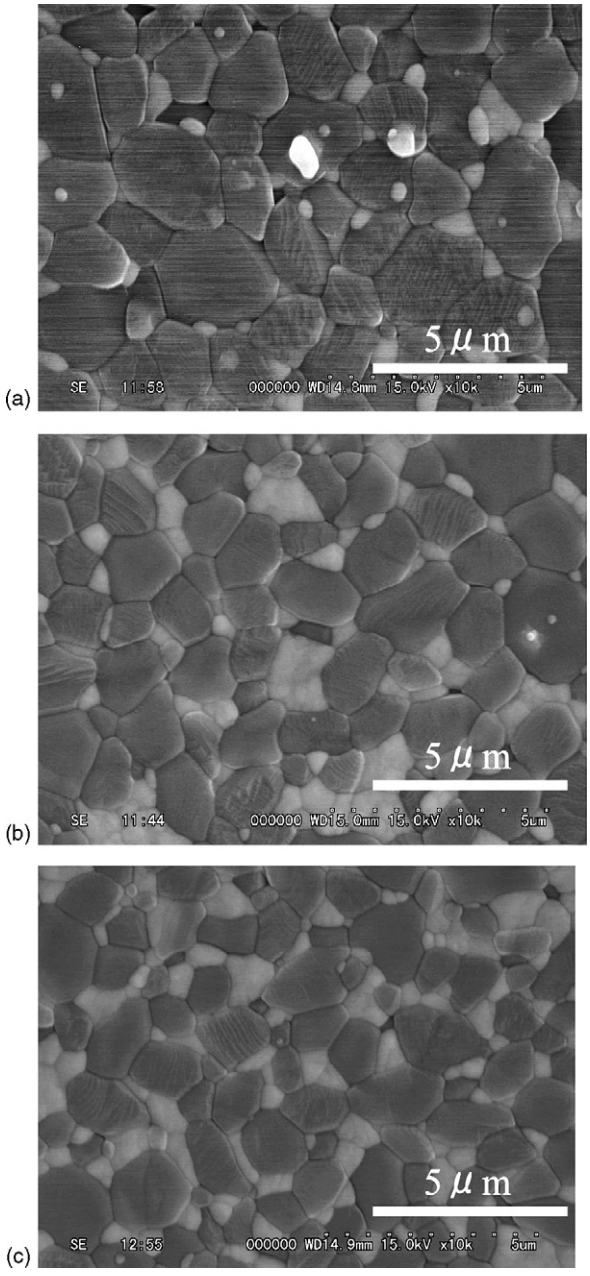

Fig. 3. SEM surface photo of alumina-based mono-foams dispersed with (a) 10 mol%, (b) 20 mol% and (c) 30 mol% of 3YSZ.

No peaks other than for alumina and zirconia are seen on XRD of the outer shell, while the peaks assigned to the silica phase can be identified on the surface of the residual silicon carbide. The silica phase probably results from the oxidation of silicon mono-oxide gas that forms during the active oxidation of silicon carbide[21] when foaming.

The grain size distribution of alumina was evaluated to confirm the grain growth suppression in detail. Fig. 4(a)–(c) plot the frequency distributions of 10, 20 and 30 mol% zirconia-dispersed alumina foams, respectively. In all cases, the maximum grain size is less than 4 μm, which means that little grain growth occurred, based on the size of the starting powders.

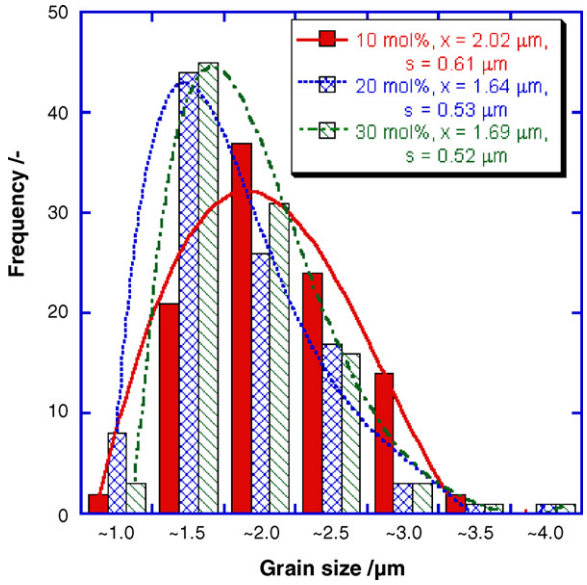

Fig. 4. Grain size distribution of alumina-based mono-foams dispersed with 10, 20 and 30 mol% of 3YSZ.

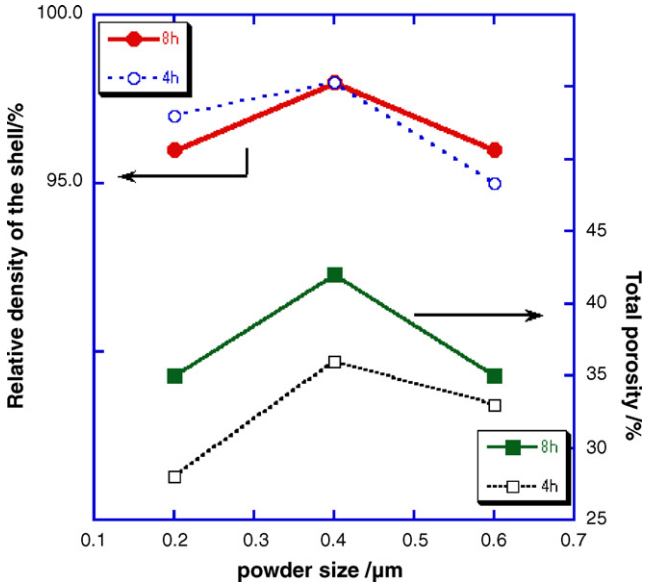

Fig. 5. Starting powder dependence of relative shell density and total porosity of alumina-based mono-foams dispersed with 30 mol% of 3YSZ.

The 30 mol% dispersed sample has a larger average grain size than the 20 mol% dispersed sample, while the 10 mol% dispersed sample has grains larger than either of the other two. The degree of foaming was maximal in the 30 mol% dispersed sample, although the grain size was not minimal.

The bond state of the grain boundary is reported to change on dispersing silica in zirconia-based ceramics.[22] Similarly, the foaming of 30 mol% dispersed alumina was enhanced due to the ductility improvement that resulted from changing the state of chemical bonding at the grain boundaries, although larger grains would hinder grain boundary sliding.

The effect of grain size on the degree of superplastic foaming was examined by varying the size of the starting alumina powder for a constant amount of dispersed 3Y. Fig. 5 shows the relative density of the outer shell and total porosity of the ceramic foams derived from 0.2-, 0.4- and 0.6-μm alumina powders added to 30 mol% 3YSZ.

In all cases, the foams treated for 8 h were higher than those treated for 4 h, which means that foaming followed sintering. The foam made from the 0.4-μm powder had the greatest outer shell density and total porosity.

The heating time dependence of the outer shell density reveals that a relatively high density (relative density >98%) was maintained in the foams made from the 0.4-μm powder, while in the foams derived from the 0.6-μm powder, the outer shell density increased with heating time, suggesting that the densification proceeded simultaneously with foaming in low density shell. Wang et al. reported that the ductility increased with decreasing relative density.[23] The relatively large deformation of the foam derived from the 0.6-μm powder on heating for 4 h was correlated with the low density of the outer shell.

For the ceramic foam derived from the 0.2-μm powder, the relative density decreased with heating time. This probably stemmed from the generation of a coarse portion resulting from insufficient ductility that was incapable of matching the expansion of the outer shell.

We initially postulated that the degree of foaming would increase with smaller starting powders due to the improved ductility. In fact, the foam height derived from the 0.2-μm powder was smaller than that from the 0.4-μm powder.

The grain size distributions of alumina-based foams made from different-sized alumina powders were examined and the results are illustrated in Fig. 6. The modal grain sized increased with the size of powder used. In the 0.2-μm-derived foam, however, there were abnormally large grains leading to a broad grain size distribution. The average grain size for foams derived from 0.4- and 0.2-μm powders was 1.68 and 1.73 μm, respectively. Consequently, the range of grain size is larger in the foams

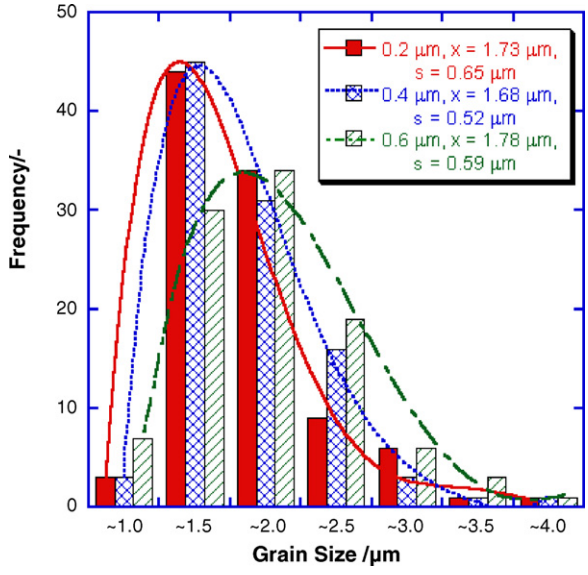

Fig. 6. Grain size distributions of alumina/3YSZ mono-foams derived from different size of starting alumina powders, heat-treated at 1600 °C for 8 h.

derived from finer powder, i.e., the standard deviation of grain size for the foams derived from 0.4- and 0.2-μm powders was 0.52 and 0.65 μm, respectively.

It has been reported that heterogeneity in microstructure leads to stress concentration resulting in insufficient superplasticity.[24] In addition to the small average grain size, the narrow grain size distribution in the foam derived from the 0.4-μm powder was advantageous in terms of the superplastic deformation leading to the largest ceramic foam.

4. Summary

We successfully fabricated alumina-based ceramic foams following sintering by improving the superplasticity by dispersing of 3YSZ or magnesia. The grain growth of alumina was suppressed by adding 3YSZ and the resultant grain size and amount of dispersion were closely related to the total porosity of the ceramic foam. Porosity of the ceramic foam depended on the grain size and their distributions irrespective of the size of starting powders.

Acknowledgements

The authors thank Sumitomo Chemical Co. Ltd., Tokyo, Japan, Tosho Corporation, Tokyo, Japan, Ube Material Industries, Ltd., Yamaguchi, Japan, for supplying α-alumina powders, yttria stabilized zirconia powders and magnesia powders, respectively.

References

1. Kishimoto, A., Higashiwada, T., Asaoka, H. and Hayashi, H., The exploitation of superplasticity in the successful foaming of ceramics following sintering. *Adv. Eng. Mater.*, in press.
2. Diaz, A., Hampshire, S., Yang, J., Ohji, T. and Kanzaki, S., Comparison of mechanical properties of silicon nitrides with controlled porosities produced by different fabrication routes. *J. Am. Ceram. Soc.*, 2005, **88**, 698–706.
3. Barea, R., Osendi, M. I., Miranzo, P. and Ferreira, J. M. F., Fabrication of highly porous mullite materials. *J. Am. Ceram. Soc.*, 2005, **88**, 777–779.
4. Gu, Y., Liu, X., Meng, G. and Peng, D., Porous YSZ ceramics by water-based gelcasting. *Ceram. Int.*, 1999, **25**, 705–709.
5. Saggio-Woyansky, J., Scott, C. E. and Minnear, W. P., Processing of porous ceramics. *Am. Ceram. Soc. Bull.*, 1992, **71**(11), 1674–1682.
6. Xie, R., Mitomo, M. and Zhan, G., Superplasticity in a fine-grained beta-silicon nitride ceramic containing a transient liquid. *Acta Mater.*, 2000, **48**, 2049–2058.
7. Albuquerque, J. M., Harmer, M. P. and Chou, Y. T., Tensile superplastic deformation of $YBa_2Cu_3O_{7-x}$ high-T_C superconductors. *Acta Mater.*, 2001, **49**, 2277–2284.
8. Nakano, K., Suzuki, T. S., Hiraga, K. and Sakka, Y., Superplastic tensile ductility enhanced by grain size refinement in a zirconia-dispersed alumina. *Scripta Mater.*, 1997, **38**, 33–38.
9. Kim, B., Hiraga, K., Sakka, Y. and Jang, B., Effect of cavitation on superplastic flow of 10% zirconia-dispersed alumina. *Scripta Mater.*, 2001, **45**, 61–67.
10. Calderon-Moreno, J. M. and Schehl, M., Microstructure after superplastic creep of alumina-zirconia composites prepared by powder alcoxide mixtures. *J. Eur. Ceram. Soc.*, 2004, **24**, 393–397.
11. Wang, J., Taleff, E. M. and Kovar, D., Superplastic deformation of Al2O3/Y-TZP particulate composites and laminates. *Acta Mater.*, 2004, **52**, 5485–5491.
12. Yoshizawa, Y. and Sakuma, T., Improvement of tensile ductility in high-purity alumina due to magnesia addition. *Acta Metall. Mater.*, 1992, **40**, 2943–2950.
13. Yoshizawa, Y. and Sakuma, T., High-temperature deformation and cavitation in fine-grained alumina. *Mater. Sci. Eng. A*, 1994, **176**, 447–453.
14. Beclin, F., Duclos, R., Crampon, J. and Valin, F., Superplasticity of HIP MgO [middle dot] Al_2O_3 spinel: prospects for superplastic forming. *J. Eur. Ceram. Soc.*, 1997, **17**, 439–445.
15. Takigawa, Y., Yoshizawa, Y. and Sakuma, T., Superplasticity in Al_2O_3-20 vol% spinel ($MgO{\cdot}1.5Al_2O_3$) 1.5ceramics. *Ceram. Int.*, 1998, **24**, 61–66.
16. Bataille, A., Crampon, J. and Duclos, R., Upgrading superplastic deformation performance of fine-grained alumina by graphite particles. *Ceram. Int.*, 1999, **25**, 215–222.
17. Kottada, R. S. and Chokshi, A. H., The high temperature tensile and compressive deformation characteristics of magnesia doped alumina. *Acta Mater.*, 2000, **48**, 3905–3915.
18. Chen, G., Zhang, K., Wang, G. and Han, W., Superplasticity in Al_2O_3-20 vol% spinel ($MgO{\cdot}1.5Al_2O_3$) ceramics. *Ceram. Int.*, 2004, **30**, 2157–2162.
19. Hiraga, K., Nakano, K., Suzuki, T. S. and Sakka, Y., Cavitation damage during high temperature tensile deformation in fine-grained alumina doped with magnesia or zirconia. *Scripta Mater.*, 1998, **39**, 1273–1279.
20. Kim, B., Hiraga, K., Morita, K. and Sakka, Y., Superplasticity in alumina enhanced by co-dispersion of 10% zirconia and 10% spinel particles. *Acta Mater.*, 2001, **49**, 887–895.
21. Narushima, T., Goto, T., Iguchi, Y. and Hirai, T., High-temperature active oxidation of chemically vapor-deposited silicon carbide in an $Ar–O_2$ atmosphere. *J. Am. Ceram. Soc.*, 1991, **74**, 2583–2586.
22. Sakuma, T., Ikuhara, Y., Takigawa, Y. and Thavorniti, P., Importance of grain boundary chemistry on the high-temperature plastic flow in oxide ceramics. *Mater. Sci. Eng. A*, 1997, **234–236**, 226–229.
23. Wang, Z. C., Davies, T. J., Ridley, N. and Ogwu, A. A., Superplasticity of ceramic materials—II. Effect of initial porosity and doping on the superplastic behaviour of alumina. *Acta Mater.*, 1996, **44**, 4301–4309.
24. Murray, N. G. D. and Dunand, D. C., Effect of thermal history on the superplastic expansion of argon-filled pores in titanium: part I kinetics and microstructure. *Acta Mater.*, 2004, **52**, 2269–2278.